

Electronic Supplementary Information

Controllable Co@N-doped graphene anchored onto the NRGO toward electrocatalytic hydrogen evolution at all pH values

Lijuan Jiang, Lijun Qiu, Tianlun Cen, Yi-Yi Liu, Xiaomin Peng, Zhifeng Ye and Dingsheng Yuan*

School of Chemistry and Materials Science, Jinan University, Guangzhou 510632, P. R. China. Email: tydsh@jnu.edu.cn

Contents

Materials and Preparation of the Catalysts.....	4
Preparation of Materials.....	4
Characterizations	4
Electrochemical Measurements.....	5
Fig. S1 SEM images of samples; (c) EDX mapping.	7
Fig. S2 SEM, TEM and HRTEM images of the different samples.....	8
Fig. S3 (a) Survey XPS spectra of the samples, (b) High-resolution XPS profiles of C 1s.	8
Fig. S4 Nyquist plots (at $\eta = 200$ mV).	10
Fig. S5 (a) SEM and (b) HRTEM images (c) XRD patterns and (d) XPS spectra of the Co@NG/NRGO initially and after the long-time durability test.....	11
Fig. S6 LSV curves before and after introducing 5.0 m M KSCN.	12
Fig. S7 LSV curves of of samples obtained by adding different amounts of melamine.	13
Fig. S8 High-resolution XPS profiles of (a) Co 2p; (b) N 1s.	14
Fig. S9 (a) LSV curves and (b) Tafel plots samples. (d) The long-term durability tests at $\eta = 150$ mV (Co@NG/NRGO) and 310 mV (Co/RGO) for HER in 0.5 M H ₂ SO ₄ electrolyte. Inset of (d) shows the C_{dl} of different materials obtained at 0.15 V versus RHE.	15
Fig. S10 (a) Polarization curves and (b) The long-term durability tests at $\eta = 400$ mV (Co@NG/NRGO) and 550 mV (Co/RGO) for HER in PBS. Inset of (d) shows Nyquist plots (at $\eta = 500$ mV).	16
Fig. S11 Mo ₂ C@NG/NRGO composites: (a) SEM image, (b) TEM image, (c) HRTEM image, (d) XRD pattern, and LSV curves in (e) 1.0 M KOH and (f) 0.5 M H ₂ SO ₄ . Inset in (e) and (f): Tafel plots.....	17
Fig. S12 Ni@NG/NRGO composites: (a) SEM image, (b) TEM image, (c) HRTEM image, (d) XRD pattern, and LSV curves in (e) 1.0 M KOH and (f) 0.5 M H ₂ SO ₄ . Insets in (e) and (f): Tafel plots.....	18
Table S1. Comparison of HER performance of carbon-based electrocatalysts.....	19
Table S2. Comparison of catalytic parameters of different HER catalysts in 1.0 M KOH.....	21
Table S3. Fitting parameters (peak area and species percentage) for four samples.	22

References 23

Materials and Preparation of the Catalysts

All chemicals were analytical grade and were used as received without further purification. All solution used in experiments were prepared with double-distilled water. The graphene oxide (GO) powder was purchased from Qitaihe Baotailong graphene New Material Co., Ltd. Cobalt-nitrate hexahydrate ($\text{Co}(\text{NO}_3)_2 \cdot 6\text{H}_2\text{O}$), melamine and potassium hydroxide (KOH) were purchased from Aladdin. Hydrazine hydrate (HCl), concentrated sulfuric acid (H_2SO_4) were purchased from Guangzhou chemical reagent factory. Phosphate buffer saline (PBS) powdered was purchased from Macklin. Ethanol (CH_3COOH) was purchased from Guangdong Guanghua Sci-Tech Co., Ltd. Nafion solution (5%) was purchased from Sigma-Aldrich.

Preparation of Materials: To prepare the Co@NG/NRGO catalyst, GO (0.2 g), $\text{Co}(\text{NO}_3)_2 \cdot 6\text{H}_2\text{O}$ (2 mmol) and melamine (2.0 g) in double-distilled water (40 mL) were sonicating for 60 min. The well-mixed precursor solution, was then freeze-dried to minimize re-stacking of the GO sheets. After drying for 24 h, the well-mixed precursor powder was obtained. After that, the thermal pyrolysis process was performed at 800°C in an Ar flow for 4 h. And finally, the Co@NG/NRGO catalyst was produced. To study the effects of thickness of graphene shell on the HER activity, the samples with different number of graphene layers were prepared by varying the adding amount of melamine, the Co@NG/NRGO-n (in which n represents the quality of melamine) was obtained by changing the amount of melamine (0.5 g, 1.0 g, 2.0 g, 3.0 g), with all the other synthetic treatments kept the same. According to a similar procedure, Co@NG was prepared from the Co precursor and melamine in the absence of GO. Co/RGO was prepared from the Co precursor and GO in the absence of melamine. NRGO was prepared as a blank from melamine and GO in the absence of the Co precursor. RGO was prepared in the absence of melamine and Co precursor.

Characterizations

SEM was performed on a ZEISS ULTRA55 instrument. TEM, HRTEM, energy dispersive spectroscopy, and elemental mapping investigations were performed with a JEOL JEM 2100F instrument. XRD analysis was performed on a Bruker D8 diffractometer using Cu K α radiation ($\lambda = 1.54056 \text{ \AA}$). XPS was processed on a PerkinElmer PHI X-tool XPS instrument, using C 1s (binding energy of 284.6 eV) as a reference. The Raman investigation was performed on a laser confocal Raman microspectrometer (XploRA, Horiba Jobin Yvon, Ltd.).

Electrochemical Measurements

The electrochemical measurements of HER was performed using an electrochemical workstation (CHI 660, CH Instruments, Inc., Shanghai, China) in a three-electrode system. As for HER test, the graphite rod was used as counter electrode, saturated calomel electrode (Hg/HgCl₂ in saturated KCl) was used as reference electrode. The synthesized samples (5 mg) were first dispersed in 1 mL of ethanol mixture and 30 μ L of 5 wt % Nafion solution prior to a ≥ 30 min sonication to form electrocatalysts ink and then loaded onto a glassy carbon electrode (GCE, 4 mm in diameter) were used as working electrodes. The potential values used in this study were changed to $E_{(RHE)}$ from $E_{(SCE)}$ according to the formula $E_{(RHE)} = E_{(SCE)} + 0.241 + 0.059 \times \text{pH}$. The HER catalytic performance of the Co@NG/NRGO samples was evaluated by linear sweep voltammetry (LSV) measurements performed in a three-electrode system (All polarization curves are not corrected for IR loss). For comparison, RGO, NRGO, Co@NG, Co/RGO, and commercial 40 wt % Pt/C with the same mass loading were also tested in alkaline electrolyte (1.0 M KOH), acidic

electrolytes (0.5 M H₂SO₄) and neutral electrolytes (1.0 M phosphate buffered saline (PBS) solution, pH = 7.4). Linear sweep voltammetry (LSV) for HER was conducted with a scan rate of 10 mV s⁻¹ in different pH electrolytes. The electrochemical impedance spectroscopy (EIS) was carried out at a specified overpotential in a frequency range from 100 kHz to 0.01 Hz and an amplitude of 5 mV.

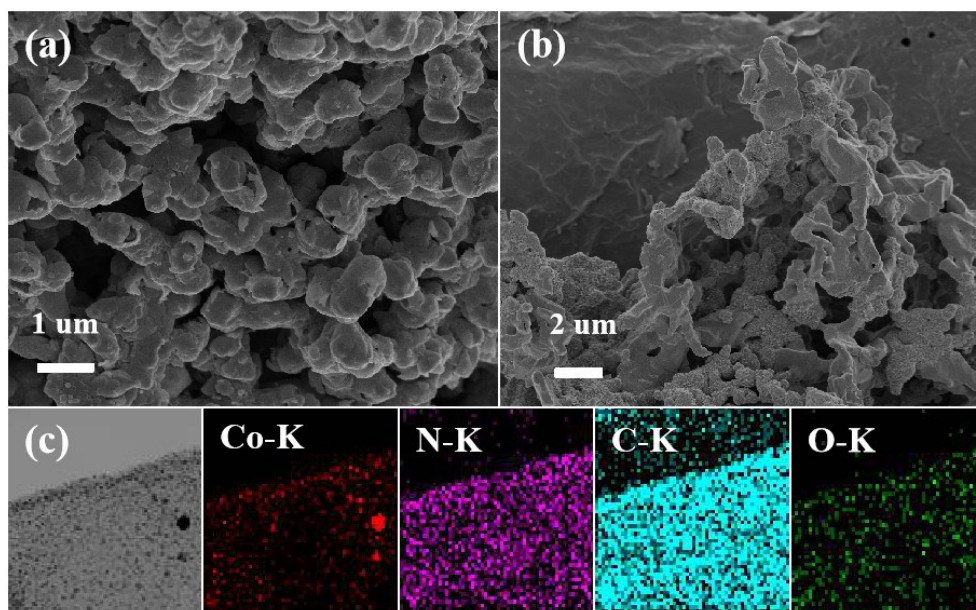


Fig. S1 SEM images of (a) Co@NG, (b) Co/RGO; (c) Corresponding EDX elemental mapping of Co, N, C and O.

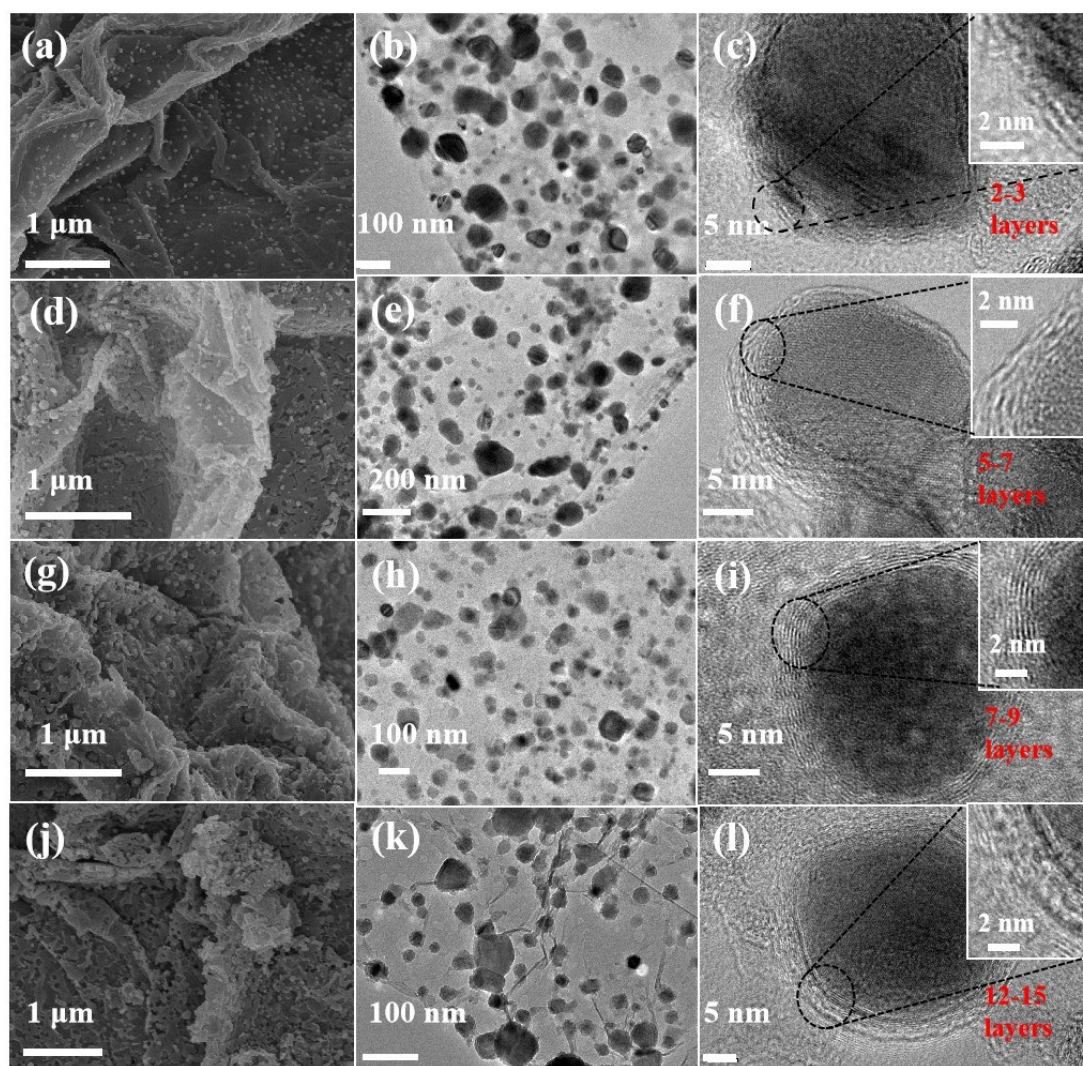


Fig. S2 (a, d, g and j) SEM, (b, e, h and k) TEM and (c, f, i and l) HRTEM images of the products obtained in the presence of melamine for (a, b and c) 0.5 g (Co@NG/NRGO-0.5), (d, e and f) 1.0 g (Co@NG/NRGO-1.0), (g, h and i) 2.0 g (Co@NG/NRGO-2.0) and (j, k and l) 3.0 g (Co@NG/NRGO-3.0).

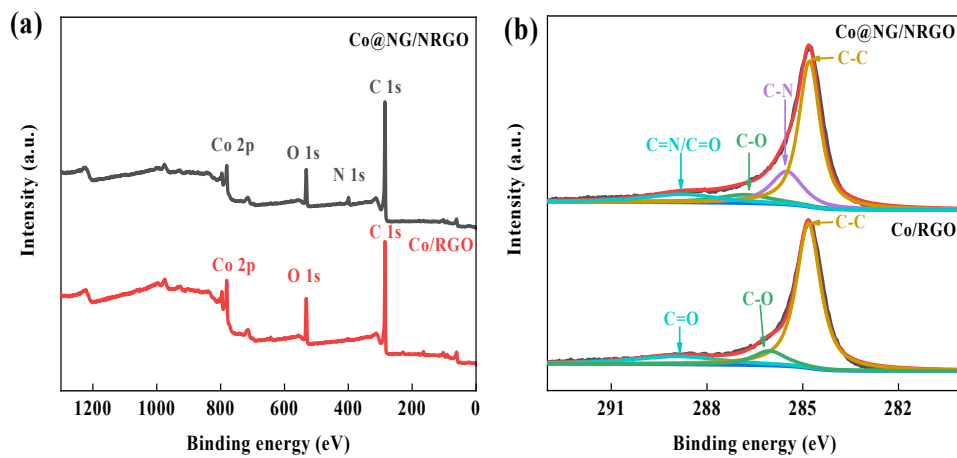


Fig. S3 (a) Survey XPS spectra of the Co@NG/NRGO and Co/RGO, (b) High-resolution XPS profiles of (b) C 1s.

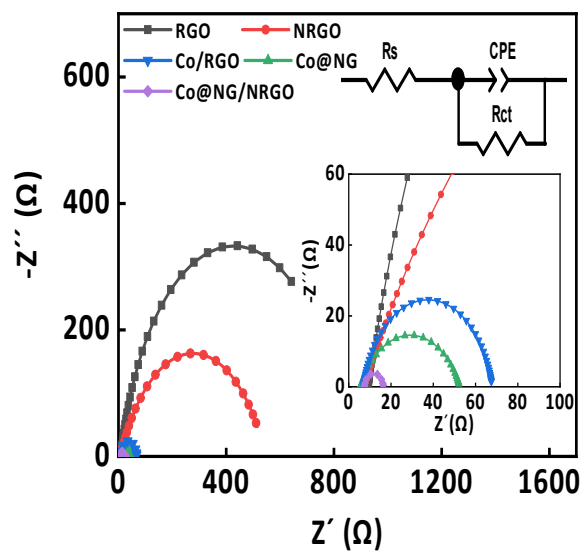


Fig. S4 Nyquist plots (at $\eta = 200$ mV).

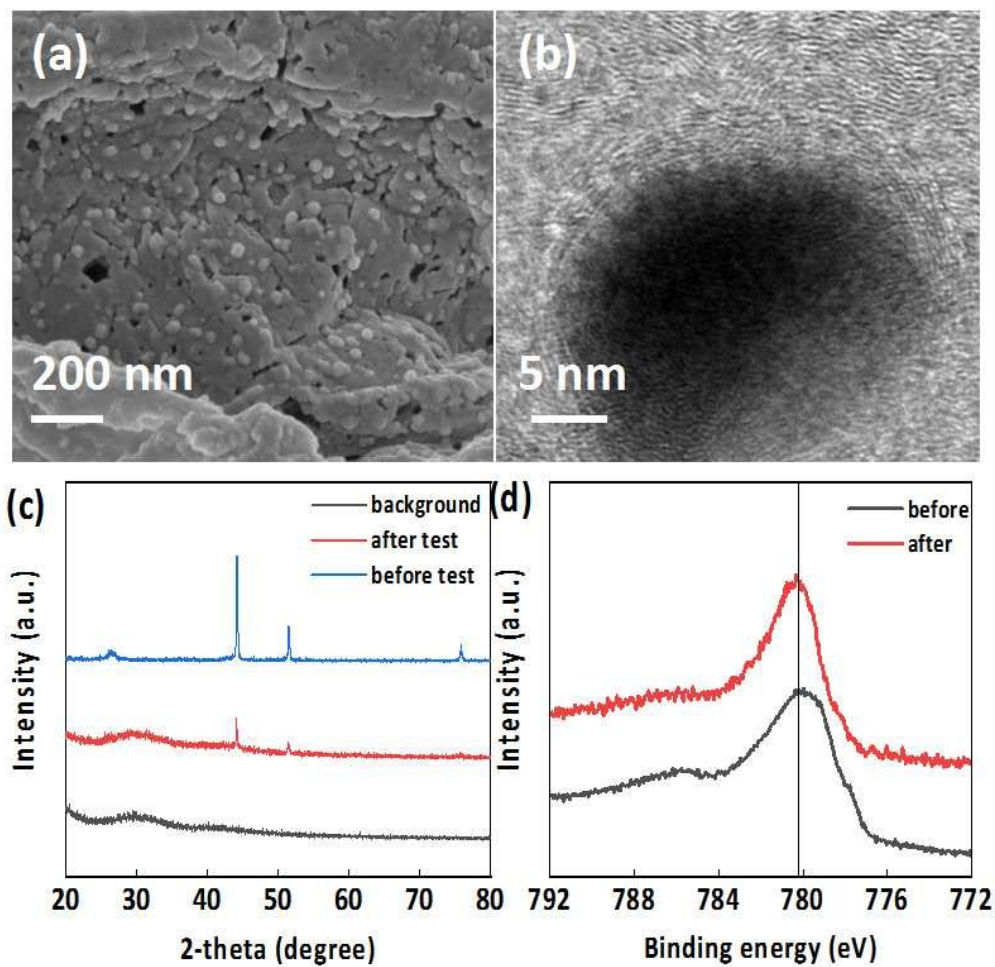


Fig. S5 (a) SEM and (b) HRTEM images of the Co@NG/NRGO initially and after the long-time durability test. (c) XRD patterns and (d) XPS spectra of the Co@NG/NRGO initially and after the long-time durability test.

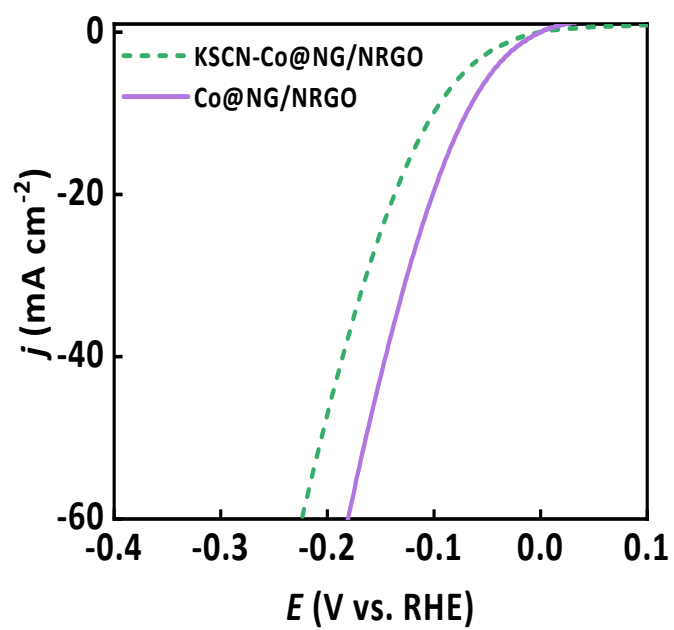


Fig. S6 Polarization curves before and after introducing 5.0 mM KSCN.

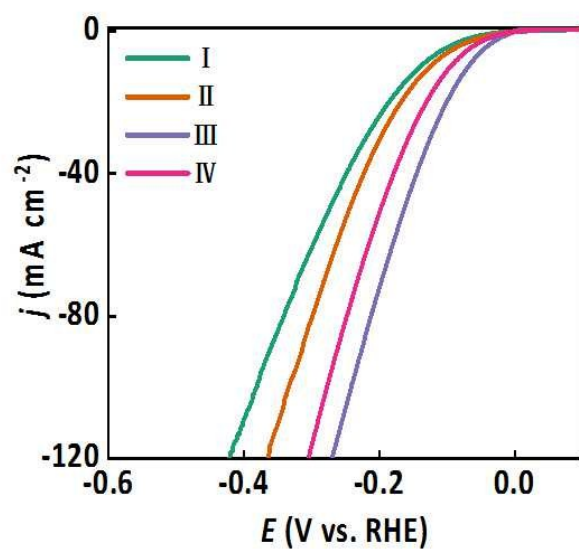


Fig. S7 Polarization curves of samples obtained by adding different amounts of melamine (I : Co@NG/NRGO-0.5, II : Co@NG/NRGO-1.0, III : Co@NG/NRGO-2.0, IV : Co@NG/NRGO-3.0). The optimized Co@NG/NRGO-2.0 sample had the best HER activity, thanks to the N-doped graphene shell regulating the electronic structure and the highest pyridinic-N and pyrrolic-N content.

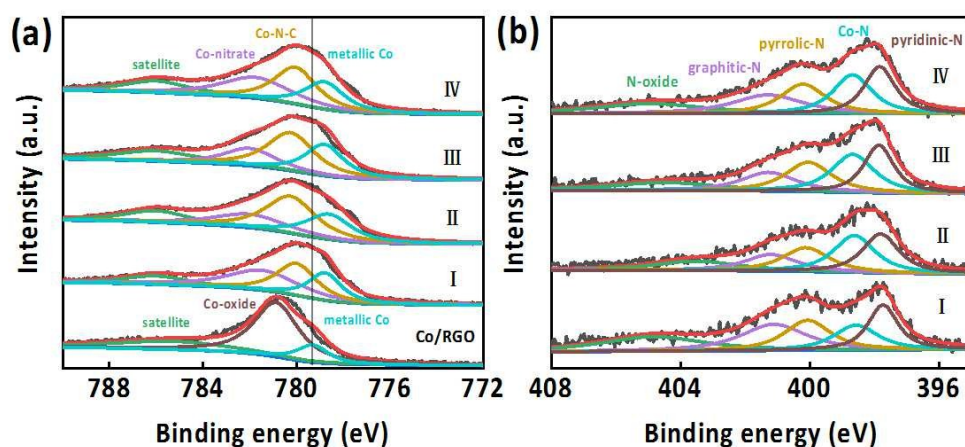


Fig. S8 High-resolution XPS profiles of (a) Co 2p; (b) N 1s. (I : Co@NG/NRGO-0.5, II : Co@NG/NRGO-1.0, III : Co@NG/NRGO-2.0, IV: Co@NG/NRGO-3.0). The introduction of N-doped graphene shells caused significant red shift of metallic Co XPS peaks in all samples, indicating the enriched electrons around Co. The penetration effect between the ultrathin graphene shells and the Co cores modulate the electron density and the electronic potential distribution and nitrogen doping can also effectively adjust the local electronic structure between Co-N bonds, improving the adsorption and desorption behaviour of proton hydrogen on the catalyst surface. And the pyridinic-N and pyrrolic-N can promote the electrical conductivity of material due to its excessive electrons.

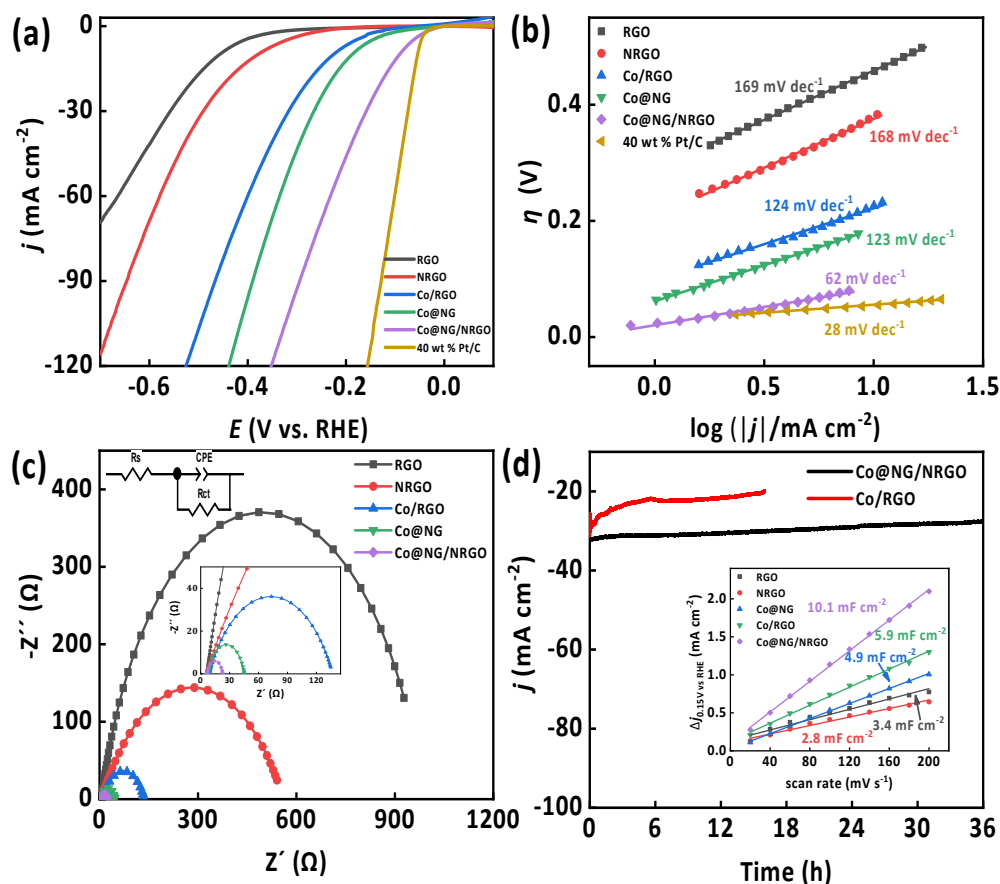


Fig. S9 (a) Polarization curves and (b) Tafel plots of RGO, NRGO, Co/RGO, Co@NG and Co@NG/NRGO. (c) Nyquist plots (at $\eta = 200$ mV). (d) The long-term durability tests at $\eta = 150$ mV (Co@NG/NRGO) and 310 mV (Co/RGO) for HER in 0.5 M H₂SO₄ electrolyte. Inset of (d) shows the C_{dl} of different materials obtained at 0.15 V versus RHE.

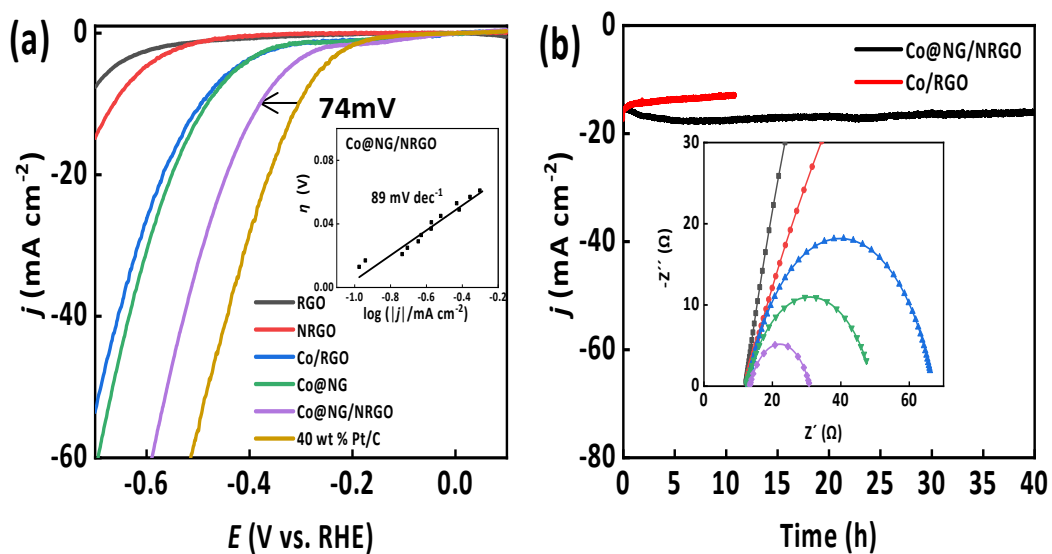


Fig. S10 (a) Polarization curves and (b) The long-term durability tests at $\eta = 400$ mV (Co@NG/NRGO) and 550 mV (Co/RGO) for HER in PBS. Inset of (a) shows Tafel plots of Co@NG/NRGO. Inset of (d) shows Nyquist plots (at $\eta = 500$ mV).

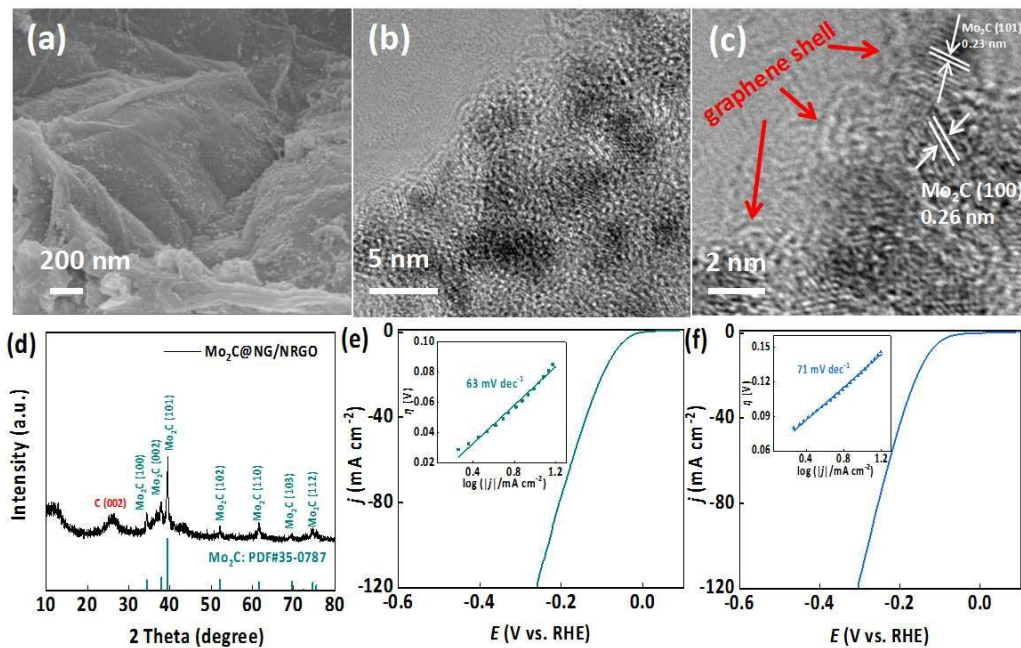


Fig. S11 Mo₂C@NG/NRGO composites: (a) SEM image, (b) TEM image, (c) HRTEM image, (d) XRD pattern, and LSV curves in (e) 1.0 M KOH and (f) 0.5 M H₂SO₄. Inset in (e) and (f): Tafel plots.

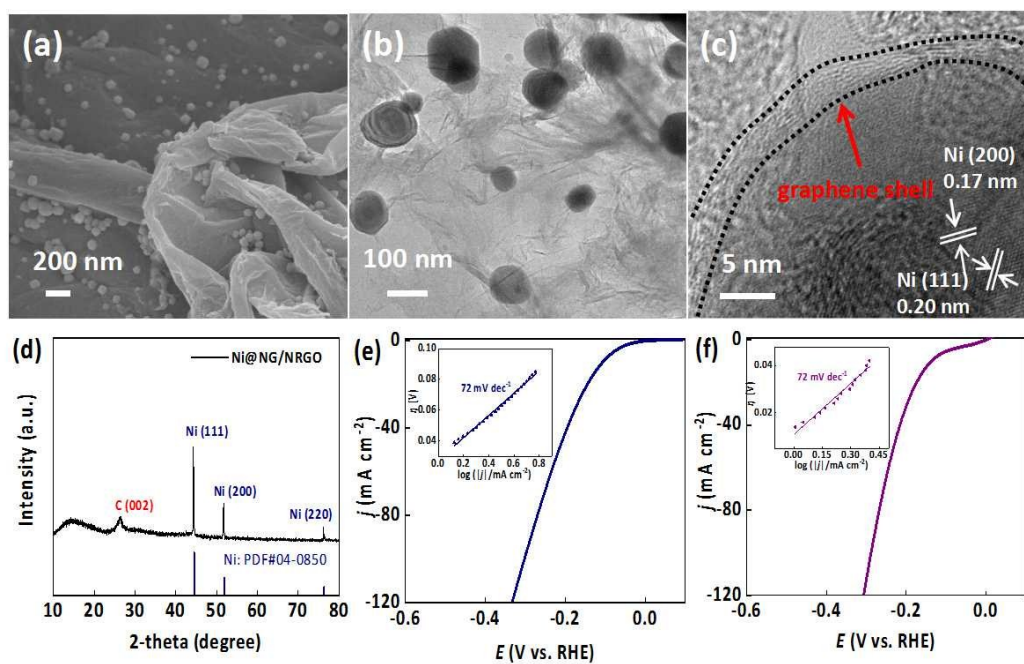


Fig. S12 Ni@NG/NRGO composites: (a) SEM image, (b) TEM image, (c) HRTEM image, (d) XRD pattern, and LSV curves in (e) 1.0 M KOH and (f) 0.5 M H₂SO₄. Insets in (e) and (f): Tafel plots.

Table S1. Comparison of HER performance for Co@NG/NRGO with other reported carbon-based electrocatalysts.

Catalyst	Electrolyte	Tafel slope (mV dec ⁻¹)	η_{10} (mV vs. RHE)	Ref.
Co@NG/NRGO	1.0 M KOH	64	70	This work
	0.5 M H ₂ SO ₄	62	91	
Co-NC	0.1 M KOH	/	266	1
	0.5 M H ₂ SO ₄	96	181	
Co@N-CNTs@rGO	1.0 M KOH	55	108	2
	0.5 M H ₂ SO ₄	52	87	
Co-NC/CNT	1.0 M KOH	125	201	3
Co-NRCNTs	0.5 M H ₂ SO ₄	80	260	4
	1.0 M KOH	/	370	
NiCoP/rGO	1.0 M KOH	124.1	209	5
	0.5 M H ₂ SO ₄	42.5	45	
CoP@BCN-1	1.0 M KOH	59	87	6
	0.5 M H ₂ SO ₄	46	150	
Co ₂ Ni ₁ N	1.0 M KOH	60.17	120.6	7
	0.5 M H ₂ SO ₄	55.30	92.0	
MoS ₂ -rGO@Mo	1.0 M KOH	62	123	8
Co-P@Co ₃ O ₄ /CC	1.0 M KOH	85	73	9
Cu ₃ P NW/CF	1.0 M KOH	67	143	10
Co _{0.1} Ni _{0.75} Se/rGO	1.0 M KOH	43	103	11
CoP@BCN-1	1.0 M KOH	52	215	12

	0.5 M H ₂ SO ₄	46	87	
P-NiCo ₂ S ₄ @CNT/CNF	1.0 M KOH	65.9	74	13
Ni@Ni(OH) ₂ /Pd/rGO	1.0 M KOH	70	76	14
CoNi@NC	1.0 M KOH	104	224	15
CoS ₂ /MoS ₂ /RGO	0.5 M H ₂ SO ₄	56	160	16
Co ₃ ZnC/RGO	0.5 M H ₂ SO ₄	83.4	/	17
CuCo@NC	0.5 M H ₂ SO ₄	79	145	18
N/Co-doped PCP/NRGO	0.5 M H ₂ SO ₄	126	229	19
CoO@Co/N-rGO	0.5 M H ₂ SO ₄	69	140	20

Table S2. Comparison of catalytic parameters of different HER catalysts in 1.0 M KOH.

Catalyst	Onset potential (mV vs RHE)	η_{10} (mV vs RHE)	j_0 (mA cm ⁻²)	Tafel slope (mV dec ⁻¹)	R_{ct} (Ω)
Pt/C	- 7	28	0.83	45	/
Co@NG/NRGO	-14	70	0.91	64	9.0
Co@NG	-121	202	0.18	109	46.6
Co/RGO	-121	222	0.11	113	60.5
NRGO	-198	314	0.081	150	508.3
RGO	-314	515	0.069	327	828.4

Table S3. Fitting parameters (peak area and species percentage) for four samples.

samples	area					Co-N (%)	pyridine-N and pyrrole-N (%)
	pyridine-N	pyrrole-N	graphite-N	Co-N	oxidized N		
Co@NG/NRGO-0.5	1325.121	1363.591	1698.398	1084.233	1501.682	17.30	42.90
Co@NG/NRGO-1.0	1632.027	1278.905	991.0138	1758.291	934.6182	27.16	44.96
Co@NG/NRGO-2.0	1762.49	1628.366	1235.698	1952.341	1038.983	27.62	47.96
Co@NG/NRGO-3.0	2022.684	1839.062	1847.172	2095.106	1550.371	23.70	43.69

The pyridinic-N and pyrrolic-N enables the fast electron transfer during the electrocatalytic HER. The quantitative XPS analysis shows the highest content of Co-N and (pyridine-N + pyrrole-N) percentage in Co@NG/NRGO-2.0 sample.

References SI

- 1 J. Chen, H. Zhou, Y. Huang, H. Yu, F. Huang, F. Zheng, S. Li, *RSC Adv.*, 2016, **6**, 42014–42018.
- 2 Z. Chen, R. Wu, Y. Liu, Y. Ha, Y. Guo, D. Sun, M. Liu, F. Fang, *Adv. Mater.*, 2018, **30**, 1802011.
- 3 F. Yang, P. Zhao, X. Hua, W. Luo, G. Cheng, W. Xing, S. Chen, *J. Mater. Chem. A*, 2016, **4**, 16057-16063.
- 4 X. Zou, X. Huang, A. Goswami, R. Silva, B. R. Sathe, E. Mikmeková, T. Asefa, *Angew. Chem. Int. Ed.*, 2014, **53**, 4372-4376.
- 5 J. Li, M. Yan, X. Zhou, Z. Huang, Z. Xia, C. Chang, Y. Ma, Y. Qu, *Adv. Funct. Mater.*, 2016, **26**, 6785-6796.
- 6 H. Tabassum, W. Guo, W. Meng, A. Mahmood, R. Zhao, Q. Wang, R. Zou, *Adv. Energy Mater.*, 2017, **7**, 1601671.
- 7 X. Feng, H. Wang, X. Bo, L. Guo, *ACS Appl. Mater. Interfaces*, 2019, **11**, 8018-8024.
- 8 B. He, L. Chen, M. Jing, M. Zhou, Z. Hou, X. Chen, *Electrochim. Acta*, 2018, **283**, 357-365.
- 9 L. Yang, H. Zhou, X. Qin, X. Guo, G. Cui, A. M. Asiri, X. Sun, *Chem. Commun.*, 2018, **54**, 2150-2153.
- 10 J. Tian, Q. Liu, N. Cheng, A. M. Asiri, X. Sun, *Angew. Chem. Int. Ed.*, 2014, **53**, 9577-9581.
- 11 W. Zhao, S. Wang, C. Feng, H. Wu, L. Zhang, J. Zhang, *ACS Appl. Mater. Interfaces*, 2018, **10**, 40491-40499.
- 12 H. Tabassum, W. Guo, W. Meng, A. Mahmood, R. Zhao, Q. Wang, R. Zou, *Adv. Energy Mater.*, 2017, **7**, 1601671.
- 13 H. Gu, W. Fan and T. Liu, *Nanoscale Horiz.*, 2017, **2**, 277-283.
- 14 Z. Deng, J. Wang, Y. Nie, Z. Wei, *J. Power Sources*, 2017, **352**, 26-33.
- 15 J. Deng, P. Ren, D. Deng, X. Bao, *Angew. Chem. Int. Ed.*, 2015, **54**, 2100-2104.
- 16 Y. Liu, X. Shang, W. Gao, B. Dong, J. Chi, X. Li, K. Yan, Y. Chai, Y. Liu, C. Liu, *App. Surf. Sci.*, 2017, **412**, 138-145.
- 17 L. Ma, X. Shen, J. Zhu, G. Zhu, Z. Ji, *J. Mater. Chem. A*, 2015, **3**, 11066-11073.
- 18 M. Kuang, Q. Wang, P. Han, G. Zheng, *Adv. Energy Mater.*, 2017, **7**, 1700193.
- 19 Y. Hou, Z. Wen, S. Cui, S. Ci, S. Mao, J. Chen, *Adv. Funct. Mater.*, 2015, **25**, 872-882.

20 X. X. Liu, J. B. Zang, L. Chen, L. B. Chen, X. Chen, P. Wu, S. Y. Zhou, Y. H. Wang, *J. Mater. Chem. A*, 2017, **5**, 5865-5872.